Radiology

ORIGINAL RESEARCH • GASTROINTESTINAL IMAGING

LI-RADS Version 2017 versus Version 2018: Diagnosis of Hepatocellular Carcinoma on Gadoxetate Disodium–enhanced MRI

Sang Min Lee, MD • Jeong Min Lee, MD • Su Joa Ahn, MD • Hyo-Jin Kang, MD • Hyun Kyung Yang, MD • Jeong Hee Yoon, MD

From the Department of Radiology, Hallym University Sacred Heart Hospital, Gyeonggi-do, Republic of Korea (S.M.L.); Department of Radiology, Seoul National University Hospital, 101 Daehak-ro, Jongno-gu, Seoul 03080, Republic of Korea (J.M.L., S.J.A., H.J.K., H.K.Y., J.H.Y.); Department of Radiology, Seoul National University College of Medicine, Seoul, Republic of Korea (J.M.L., J.H.Y.); Institute of Radiation Medicine, Seoul National University Medical Research Center, Seoul, Republic of Korea (J.M.L.); and Department of Medical Imaging, Saint Michael's Hospital, University of Toronto, Toronto, ON, Canada (H.K.Y.). Received December 18, 2018; revision requested February 11, 2019; revision received May 8; accepted May 29. **Address correspondence to** J.M.L. (e-mail: *jmsh@snu.ac.kr*).

Conflicts of interest are listed at the end of this article.

Radiology 2019; 292:655–663 • https://doi.org/10.1148/radiol.2019182867 • Content codes: GI MR OI

Background: Few studies have reported on the diagnostic performance of Liver Imaging Reporting and Data System (LI-RADS) LR-5 or LR-5 V in the diagnosis of hepatocellular carcinoma (HCC) using MRI with gadoxetate disodium.

Purpose: To determine the diagnostic performance of LI-RADS version 2018 (hereafter, v2018) on gadoxetate disodium–enhanced MRI in comparison with LI-RADS version 2017 (hereafter, v2017) for the diagnosis of HCC in patients with cirrhosis or chronic hepatitis B viral infection or at high risk for HCC.

Materials and Methods: This retrospective study between January 2013 and October 2015 evaluated consecutive patients at high risk for HCC who had at least one observation of 10 mm or greater on gadoxetate disodium–enhanced MRI and no history of previous treatment for hepatic lesions. MRI features were reviewed by three radiologists. Observations were categorized according to LI-RADS v2018 and LI-RADS v2017. Per-observation sensitivity and specificity of LR-5 using LI-RADS v2017 and v2018 were compared using generalized estimating equation models.

Results: A total of 422 observations, including 234 HCCs confirmed by results of pathologic examination in 387 patients (305 men and 82 women; mean age ± standard deviation, 59 years ± 10), were included. In all observations, LI-RADS v2018 provided higher sensitivity than LI-RADS v2017 (81% [189 of 234] vs 68% [160 of 234], respectively; $P < .001$). In small observations (10–19 mm), LI-RADS v2018 yielded much higher sensitivity than LI-RADS v2017 (76% [34 of 45] vs 11% [five of 45], respectively; $P < .001$) with relatively little impairment of specificity (94% [121 of 128] vs 99% [127 of 128], respectively; $P = .013$).

Conclusion: Updated LR-5 criteria of Liver Imaging Reporting and Data System (LI-RADS) version 2018 on gadoxetate disodium–enhanced MRI can improve sensitivity in the diagnosis of small hepatocellular carcinomas (10–19 mm) with only slight impairment in specificity compared with the criteria of LI-RADS version 2017.

Online supplemental material is available for this article.

Hepatocellular carcinoma (HCC) can be noninvasively diagnosed based on imaging features without biopsy in patients with cirrhosis or chronic liver disease, owing to the high pretest probability of HCC (1). The current clinical practice guidelines from major scientific organizations or societies suggest that a nodule 1 cm or larger with typical imaging features at dynamic CT or MRI can be noninvasively diagnosed as HCC with high specificity in high-risk patients (1,2). Yet, until the Liver Imaging Reporting and Data System (LI-RADS) was released in 2011 by the American College of Radiology, there was no consistent reporting system and standardized terminologies for the interpretation of imaging features on HCC imaging systems; therefore, there was an increased clinical demand for structured imaging reporting systems (3).

LI-RADS is widely accepted as a good scheme for interpreting and reporting imaging features of liver nodules at CT and MRI in patients at high risk for HCC, enabling the categorization of observations from LR-1 (definitely benign) to LR-5 (definitely HCC), depending on the probability of benignity or HCC (4–6). LI-RADS version 2018 (hereafter, v2018) represents the fourth update of this HCC imaging system after its first release in 2011. It has two major changes in threshold growth definition (size increase of a mass by ≥ 50% in ≤ 6 months) and LR-5 criteria. These changes were made to achieve simplicity and close concordance with the American Association for the Study of Liver Diseases (AASLD) and Organ Procurement and Transplantation Network criteria (7). In LI-RADS v2018, the requirement for antecedent visibility at US has been removed. Also, a 10–19-mm observation with nonrim arterial phase hyperenhancement (APHE) and one additional major feature, including nonperipheral "washout" and threshold growth, is now categorized as LR-5 (categorized as LR-4 in LI-RADS version 2017 [hereafter, v2017]).

Prior studies have reported the diagnostic performance of the LR-5 or LR-5 V criteria of LI-RADS version 2014

Abbreviations

AASLD = American Association for the Study of Liver Diseases, APHE = arterial phase hyperenhancement, cHCC-CCA = combined HCC-cholangiocarcinoma, ECA = extracellular agent, HCC = hepatocellular carcinoma, LI-RADS = Liver Imaging Reporting and Data System, NPV = negative predictive value, PPV = positive predictive value

Summary

Liver Imaging Reporting and Data System (LI-RADS) version 2018 with updated LR-5 criteria improves sensitivity for the diagnosis of small (10–19 mm) hepatocellular carcinomas on gadoxetate disodium–enhanced MRI compared with LI-RADS version 2017.

Key Points

- Liver Imaging Reporting and Data System version 2018 had higher sensitivity for categorization of hepatocellular carcinomas (HCCs) as LR-5 on gadoxetate disodium–enhanced MRI compared with LI-RADS version 2017 (81% [189 of 234] vs 68% [160 of 234], respectively; $P < .001$).
- For the diagnosis of small HCCs (10–19 mm), LI-RADS version 2018 had higher sensitivity than LI-RADS version 2017 (76% [34 of 45] vs 11% [five of 45], respectively; $P < .001$).
- LR-5 criteria of LI-RADS version 2018 had lower specificity than LI-RADS version 2017 for diagnosis of small HCCs (10–19 mm) (94% [121 of 128] vs 99% [127 of 128], respectively; $P = .013$).

or v2017 in the diagnosis of HCC using CT or MRI with extracellular contrast agents (ECAs) (8–14), but few studies have reported the diagnostic performance of LI-RADS using MRI with gadoxetate disodium (12–16). Several studies have demonstrated that LR-5 or LR-5 V criteria provided high specificity but low sensitivity, especially in the diagnosis of small HCCs using MRI with either ECA or gadoxetate disodium (8,9,15,16). Low sensitivity may indicate continued need for a histopathologic diagnosis via biopsy (17,18).

Furthermore, previous studies have reported that LI-RADS would not be better than AASLD for the diagnosis of small HCCs, owing to its strict diagnostic criteria (8,16). On the other hand, the updated LR-5 criteria of LI-RADS v2018 are more closely concordant with AASLD, and thus are expected to provide improved diagnostic performance compared with prior versions of LI-RADS. However, LI-RADS v2018 has not been validated widely (19–21).

The aim of our study, therefore, was to determine the diagnostic performance of the updated LR-5 criteria of LI-RADS v2018, in comparison with LI-RADS v2017, for the diagnosis of HCC in high-risk patients using MRI with gadoxetate disodium.

Materials and Methods

This retrospective cohort study was approved by the Institutional Review Board of Seoul National University Hospital and the requirement of written informed consent was waived.

Patient Studies

From January 2013 to October 2015, we identified 6156 consecutive patients who underwent gadoxetate disodium–enhanced MRI for surveillance of HCC or suspected hepatic tumors at US or CT in the picture archiving and communication system (M-view; Infinitt Health Care, Seoul, South Korea) of Seoul National University Hospital. Two radiologists (J.M.L. and S.M.L., with 25 and 10 years of experience in abdominal MRI, respectively) reviewed the electronic medical records, radiologic reports, and MRI scans of these patients to determine their eligibility. A hepatic observation was defined as an area distinct from the background liver detected on any phase of the routine MRI sequences (22). The inclusion criteria were as follows: *(a)* age of 18 years or older; *(b)* high risk for HCC according to LI-RADS v2017 (cirrhosis or chronic hepatitis B viral infection [Appendix E1 {online}]); *(c)* at least one hepatic observation 10 mm or larger, except hepatic cysts, on MRI with gadoxetate disodium; and *(d)* no previous treatment for hepatic lesions. Exclusion criteria were as follows: *(a)* no observations (≥ 10 mm) other than hepatic cysts on MRI and *(b)* congestive hepatopathies, such as Budd-Chiari syndrome, chronic portal vein occlusion, hereditary hemorrhagic telangiectasis, and cardiac congestion. Accordingly, we included 935 patients. Thereafter, the same two radiologists (J.M.L. and S.M.L.) reviewed the imaging studies and pathologic reports of the 935 patients and selected and annotated target observations (≤ 3 observations per patient) at MRI after excluding those with an insufficient final diagnosis (eg, histopathologic diagnosis more than 2 months after the MRI examination, inconclusive histopathologic diagnosis, immediate local treatment, and insufficient follow-up to determine size stability), MRI image degradation or omission, and duplicated data. Of the patients, 29 patients had been included in a previous study (23).

MRI Acquisition

All patients underwent gadoxetate disodium–enhanced MRI examinations using either a 1.5-T (Signa HDxt; GE Medical Systems, Milwaukee, Wis) (n = 135) or 3-T MRI scanner (Discovery MR750w, GE Medical Systems; Magnetom Verio, Magnetom Trio, Magnetom Skyra, Biograph mMR; Siemens Healthineers, Erlangen, Germany; and Ingenia, Philips Medical System, Best, the Netherlands) (n = 252). Routine MRI sequences included T2-weighted, diffusion-weighted, unenhanced T1-weighted imaging, dynamic imaging, and hepatobiliary phase imaging using gadoxetate disodium (Primovist; Bayer AG, Leverkusen, Germany). Details of MRI with gadoxetate disodium are presented in Appendix E2 (online) and Table E1 (online).

Image Analysis

Three abdominal imaging radiologists (H.J.K., H.K.Y., and S.J.A., with 1 year, 1 year, and 3 years of postfellowship experience in abdominal imaging, respectively) independently assessed all MRI scans. All three were blinded to the final diagnosis of each observation, but were informed that the study population consisted of HCCs, non-HCC malignancies, and benign lesions in high-risk patients. Prior to starting the image reviews, we provided the readers with self-learning material, including representative lesions for each imaging feature as well as a brief lecture based on the LI-RADS v2017 core. Thereaf-

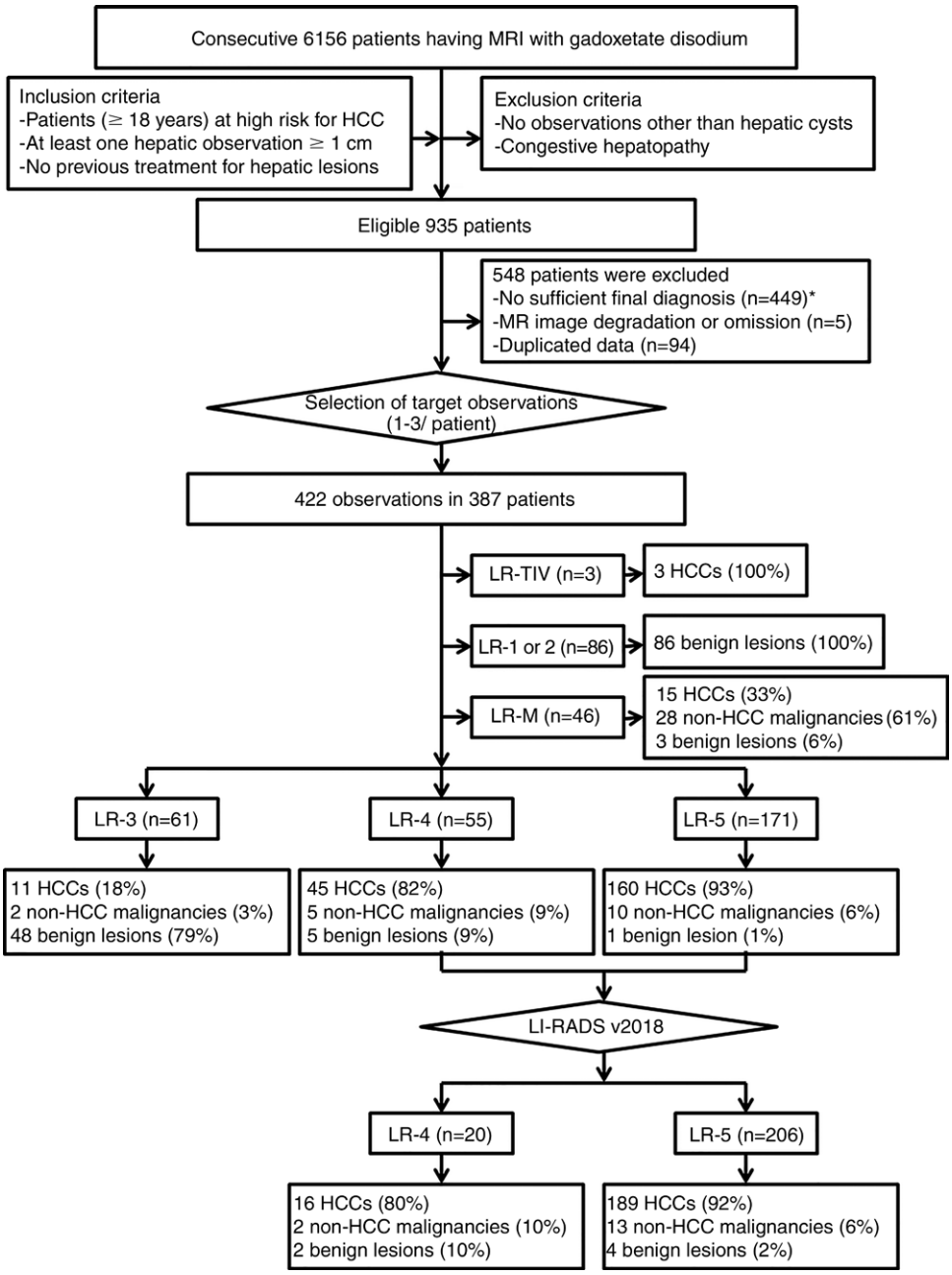

Figure 1: Flow diagram of the study sample. HCC = hepatocellular carcinoma, LI-RADS = Liver Imaging Reporting and Data System. * = Patients with insufficient final diagnoses (*n* = 449) included patients with a histopathologic diagnosis more than 2 months after MRI examination (*n* = 35), inconclusive histopathologic diagnosis (*n* = 13), immediate local treatment or systemic therapy without pathologic diagnosis (*n* = 337), and insufficient follow-up to determine size stability (*n* = 64).

ter, the readers reviewed the MRI features of the 422 observations annotated on the MRI. The readers were allowed to use all routine MRI sequences, including hepatobiliary phase and diffusion-weighted imaging. According to the LI-RADS diagnostic algorithm as the index test in our study, they initially determined if the observations were categorized as LR- TIV (definite tumor in vein), LR-1 or LR-2 (definitely or probably benign), or LR-M (probably or definitely malignant but not HCC specific) using the consensus method (Appendix E3 [online]). The three readers then evaluated the presence or absence of major features (APHE, washout, and enhancing "capsule") (Table E2 [online]). LR-TIV, LR-1 or 2, LR-M, and all MRI features were defined based on LI-RADS v2017 (22). Observations showing any targetoid mass appearance or the infiltrative appearance were regarded as LR-M (Appendix E4 [online], Table E2 [online]).

After excluding observations assigned to LR-TIV, LR-1 or 2, or LR-M, we determined the final LI-RADS categorization from LR-3 to LR-5 by using the observation size and major features, including APHE, washout, and enhancing capsule, but not including threshold growth and visibility at screening US. Final categorizations were determined by using per-reader data and consensus data. Thereafter, further categorization into LR-4 and LR-5 was performed, applying the new LR-5 criteria in LI-RADS v2018. According to LI-RADS v2018, 10–19-mm observations showing APHE and washout were classified into LR-5, which had previously been categorized as LR-4 in LI-RADS v2017 (Fig E1 [online]). Category adjustment on applying ancillary features or the tiebreaking rule was not considered when observations were categorized from LR-3 to LR-5.

Only LR-5 was regarded as a noninvasive definite diagnosis of HCC to determine the diagnostic performance of LI-RADS v2017 and v2018 (10,24).

Reference Standard

The reference standard for a hepatic diagnosis was based on pathology findings obtained by surgical resection or percutaneous biopsy. Percutaneous biopsy was performed by using an 18-gauge automatic gun under US guidance. However, most benign lesions did not require pathologic confirmation in the clinical setting, except when the imaging features were atypical. Thus, clinical diagnosis including typical imaging features (25–29) with size stability (≥ 2 years), as well as pathology findings, were regarded as reference standards for benign lesions.

Table 1: Clinical-pathologic Characteristics of Patients and Lesions

Characteristic	Value
Patient (n = 387)	
Mean age (y)*	59 ± 10
Sex	
Men	305
Women	82
Known cirrhosis	287 (74)
Cause of liver disease	
Hepatitis B virus	347 (90)
Hepatitis C virus	12 (3)
Hepatitis B and C virus	9 (2)
Alcohol	6 (2)
Other cause	13 (3)
No. of observations per patient	
1	367 (95)
2	18 (4)
3	2 (1)
Final diagnosis	
HCC	224 (58)
Non-HCC malignancies	42 (11)
Benign lesions	121 (31)
Lesion (n = 422)	
Median size (mm)†	24 (25)
HCC	31 (24)
Non-HCC malignancies	38 (41)
Benign lesions	13 (5)
Size subgroup	
10–19 mm	173 (41)
≥20 mm	249 (59)
Standard reference of diagnosis	
Pathologic diagnosis	297 (70)
Typical imaging features with size stability (≥ 2 years)‡	125 (30)
Final diagnosis	
HCC	234 (55)
Non-HCC malignancy	45 (11)
IMCC	24 (54)
cHCC-CCA	15 (33)
Metastasis	6 (13)
Benign lesion	143 (34)
Median time interval between MRI and pathologic diagnosis (d)†	10 (19)

Note.—Unless stated otherwise, data are number of patients or observations. Data in parentheses are percentages. cHCC-CCA = combined HCC-cholangiocarcinoma, HCC = hepatocellular carcinoma, IMCC = intrahepatic mass-forming cholangiocarcinoma.

* Data are mean ± standard deviation.

† Data are presented as median values. Data in parentheses are interquartile range and were calculated as the difference between the 75th and 25th percentiles.

‡ Only for diagnosis of benign lesions.

Statistical Analysis

For the diagnosis of HCC, we calculated the sensitivity, specificity, positive predictive value (PPV), and negative predictive value (NPV) with 95% confidence intervals of LR-5 in LI-RADS v2017 and LI-RADS v2018 for all observations and for a subgroup of small observations (10–19 mm) by using consensus data and per-reader data. We compared the sensitivity and specificity of LI-RADS v2017 and v2018 by using the generalized estimating equation model so as to avoid patient cluster effects. To evaluate interreader agreement, Fleiss kappa values were used for LI-RADS categories and major features and weighted kappa values were used for overall LI-RADS categories. A higher kappa value suggests stronger agreement. Interpretation of kappa values was as follows: poor, less than 0.00; slight, 0.00–0.20; fair, 0.21–0.40; moderate, 0.41–0.60; substantial, 0.61–0.80; and almost perfect, 0.81–0.99 (30). Statistical analyses were performed by using commercially available software (MedCalc Software version 18.11.3, Mariakerke, Belgium; or SPSS version 24, IBM, Armonk, NY) and free software (R version 3.5.1; R Foundation for Statistical Computing, Vienna, Austria), with a P value of less than .05 considered indicative of a statistically significant difference.

Results

Patients and Hepatic Observations

We included 422 observations (≥ 10 mm) in 387 patients in our final analysis (Fig 1). The clinical-pathologic characteristics of the patients (305 men and 82 women; mean age, 59 years) are described in Table 1. Most patients (74% [287 of 387]) had cirrhosis and the most common cause of liver disease was the hepatitis B virus (90% [347 of 387]). The number of observations per patient was one in 95% (367 of 387) of the patients and two or three in the remaining patients. Of the 422 observations (median size, 24 mm), 41% (173 of 422) were 10–19 mm in size. Fifty-five percent (234 of 422) of the observations were confirmed as HCCs, 11% (45 of 422) as non-HCC malignancies, and 34% as benign lesions (143 of 422). The 45 non-HCC malignancies included 24 (54%) intrahepatic mass-forming cholangiocarcinomas, 15 (33%) combined HCC-cholangiocarcinomas (cHCC-CCAs), and six (13%) metastases; all six metastatic adenocarcinomas originated from the colon. Of the benign lesions, 87% (125 of 143) were diagnosed by typical imaging features demonstrating size stability for at least 2 years (Table E3 [online]).

Diagnostic Performance of LR-5 of LI-RADS v2017

The per-observation diagnostic accuracy of LR-5 using LI-RADS v2017 for the diagnosis of HCC using the consensus data and per-reader data is summarized in Table 2 and Table E4 (online). The sensitivity, specificity, PPV, and NPV of LR-5 for the diagnosis of HCC were 68% (160 of 234), 94% (177 of 188), 93% (160 of 171), and 70% (177 of 251), respectively. For small observations (10–19 mm), sensitivity, specificity, PPV, and NPV were 11% (five of 45), 99% (127 of 128), 83% (five of six), and 76% (127 of 167), respectively. The per-patient diagnostic performance of LR-5 using LI-RADS v2017 for the diagnosis of HCC is listed in Table E5 (online).

According to LI-RADS v2017, 1% (three of 422), 20% (86 of 422), 11% (46 of 422), 14% (61 of 422), 13% (55 of 422),

Table 2: Diagnostic Performance for LR-5 in the Diagnosis of Hepatocellular Carcinoma Using Consensus Data

	All Lesions (n = 422)			10–19-mm Lesions (n = 173)		
Variable	LI-RADS Version 2017	LI-RADS Version 2018	*P* Value	LI-RADS Version 2017	LI-RADS Version 2018	*P* Value
Sensitivity (%)	68 (160/234) [62.0, 74.3]	81 (189/234) [75.1, 85.6]	<.001	11 (5/45) [3.7, 24.1]	76 (34/45) [60.5, 87.1]	<.001
Specificity (%)	94 (177/188) [89.8, 97.0]	91 (171/188) [85.9, 94.6]	.013	99 (127/128) [95.7, 100.0]	94 (121/128) [89.1, 97.8]	.013
Positive predictive value (%)	93 (160/171) [89.1, 96.3]	92 (189/206) [87.6, 94.6]	NA	83 (5/6) [37.5, 97.7]	83 (34/41) [69.9, 91.1]	NA
Negative predictive value (%)	70 (177/251) [66.4, 74.3]	79 (171/216) [74.4, 83.2]	NA	76 (127/167) [74.1, 77.9]	92 (121/132) [86.8, 94.9]	NA
No. of true-positive findings	160	189	NA	5	34	NA
No. of false-negative findings	74	45	NA	40	11	NA
No. of false-positive findings	11	17	NA	1	7	NA
No. of true- negative findings	177	171	NA	127	121	NA

Note.—Data in parentheses were used to calculate percentages. Data in brackets are 95% confidence intervals. *P* values were calculated by using generalized estimating equations. Diagnostic performance of LR-5 in diagnosing hepatocellular carcinomas by using per-reader data are shown in Table E4 (online). LI-RADS = Liver Imaging Reporting and Data System, NA = not applicable.

a. b. c.

Figure 2: Axial images of gadoxetate-enhanced MRI in a 62-year-old man with chronic hepatitis B and hepatocelluar carcinoma (HCC). **(a)** Arterial phase image, **(b)** portal venous phase image, and **(c)** transitional phase image of T1-weighted three-dimensional gradient-echo images show a 30-mm observation in segment 7 of the liver. The observation shows **(a)** arterial phase hyperenhancement (arrow) and **(b)** washout (arrow) on portal venous phase. No enhancing capsule was shown on **(b)** portal venous phase and **(c)** transitional phase. This hepatic observation was classified as LR-5 and confirmed as HCC by surgical resection.

and 41% (171 of 422) of all observations were categorized as LR-TIV, LR-1 or 2, LR-M, LR-3, LR-4, and LR-5, respectively (Fig 1). Ninety-three percent (160 of 171) of observations categorized as LR-5 were HCCs (Fig 2). Interreader agreements and distributions of LI-RADS categories are listed in Table 3. In observations excluding LR-TIV, LR-1 or LR-2, and LR-M, interreader agreements and frequencies of major features and combination of major features are presented in Table E6 (online) and Table 4, respectively.

Diagnostic Performance of LR-5 of LI-RADS v2018

The diagnostic accuracy of LR-5 using LI-RADS v2018 for the diagnosis of HCC is summarized in Table 2 and Table E4 (online). The sensitivity, specificity, PPV, and NPV of LR-5 for the diagnosis of HCC were 81% (189 of 234), 91% (171 of 188), 92% (189 of 206), and 79% (171 of 216), respectively. In the subgroup of small observations (10–19 mm), the sensitivity, specificity, PPV, and NPV were 76% (34 of 45), 94% (121 of 128), 83% (34 of 41), and 92% (121 of 132), respectively. The per-patient diagnostic performance of LR-5 using LI-RADS v2018 for the diagnosis of HCC is listed in Table E5 (online).

LR-5 using LI-RADS v2018 provided higher sensitivity than that using LI-RADS v2017 in the diagnosis of HCC (81% [189 of 234] vs 68% [160 of 234], respectively; $P <$ .001). In particular, in the diagnosis of small HCCs (10–19 mm), the sensitivity of LR-5 improved from 11% ([five of 45], LI-RADS v2017) to 76% ([34 of 45], LI-RADS v2018) ($P <$ .001) (Fig 3). LR-5 using LI-RADS v2018 also provided high specificity (> 90%), although it was lower than that of LR-5 using LI-RADS v2017 in all observations and in a subgroup of 10–19-mm observations (P = .013 for both).

According to LI-RADS v2018, 64% (35 of 55) of LR-4 observations using v2017 were recategorized as LR-5 (Fig 1). Twenty-nine small HCCs showing APHE and washout were

Table 3: Inter-reader Agreements and Distributions of LI-RADS Categories

Category	Kappa Value	All Observations (n = 422) Total	HCC (n = 234)	Non-HCC Malignancies (n = 45)	Benign Lesions (n = 143)	10–19 mm Observations (n = 173) Total	HCC (n = 45)	Non-HCC Malignancies (n = 8)	Benign Lesions (n = 120)
LR-TIV	0.28	3	3 (100)	0 (0)	0 (0)	0	0 (0)	0 (0)	0 (0)
LR-1 or LR-2	0.60	86	0 (0)	0 (0)	86 (100)	69	0 (0)	0 (0)	69 (100)
LR-M	0.56	46	15 (33)	28 (61)	3 (6)	4	0 (0)	3 (75)	1 (25)
LR-3	0.46	61	11 (18)	2 (3)	48 (79)	57	9 (16)	2 (3)	46 (81)
LR-4	0.62	55	45 (82)	5 (9)	5 (9)	37	31 (84)	3 (8)	3 (8)
LR-5	0.73	171	160 (93)	10 (6)	1 (1)	6	5 (83)	0 (0)	1 (17)
Overall (v2017)	0.62		NA	NA	NA		NA	NA	NA
LR-4 (v2018)	0.29	20	16 (80)	2 (10)	2 (10)	2	2 (100)	0 (0)	0 (0)
LR-5 (v2018)	0.69	206	189 (92)	13 (6)	4 (2)	41	34 (83)	3 (7)	4 (10)
Overall (v2018)	0.60		NA	NA	NA		NA	NA	NA

Note.—Data in parentheses are percentages. The Fleiss kappa value of each Liver Imaging Reporting and Data System (LI-RADS) category for three readers was calculated. Overall (v2017 or v2018) = weighted kappa value for overall categorization using LI-RADS version 2017 or version 2018, respectively; LR-4 (v2018) = LR-4 categorized according to LI-RADS version 2018; LR-5 (v2018) = LR-5 categorized according to LI-RADS version 2017. HCC = hepatocellular carcinoma, NA = not applicable.

Table 4: Combination of Major Features in Observations from LR-3 to LR-5

Category and Feature	No. of Observations	HCC (n = 234)	Non-HCC Malignancy (n = 45)	Benign Lesion (n = 143)
LR-3 (n = 61)				
≥20 mm, no APHE + no additional major feature*	4	2 (50)	0 (0)	2 (50)
10–19 mm, APHE + no additional major feature	15	4 (27)	2 (13)	9 (60)
10–19 mm, no APHE + washout	14	3 (21)	0 (0)	11 (79)
10–19 mm, no APHE + enhancing capsule	1	0 (0)	0 (0)	1 (100)
LR-4 (n = 55)				
≥20 mm, APHE + no additional major feature	9	9 (100)	0 (0)	0 (0)
≥20 mm, no APHE + washout	9	5 (56)	2 (22)	2 (22)
10–19 mm, APHE + washout†	35	29 (82)	3 (9)	3 (9)
10–19 mm, APHE + enhancing capsule	2	2 (100)	0 (0)	0 (0)
LR-5 (n = 171)				
≥20 mm, APHE + washout + enhancing capsule†	44	43 (98)	1 (2)	0 (0)
≥20 mm, APHE + washout†	121	112 (93)	9 (7)	0 (0)
10–19 mm, APHE + washout + enhancing capsule†	6	5 (83)	0 (0)	1 (17)

Note.—Data are number of observations. Data in parentheses are percentages. APHE = arterial phase hyperenhancement, HCC = hepatocellular carcinoma.

* Additional major features, including washout and an enhancing capsule.

† These combinations of major features meet the LR-5 criteria in Liver Imaging Reporting and Data Systems v2018.

additionally categorized as LR-5 by using LI-RADS v2018 (Fig 3, Table 4). However, false-positive results increased from 11 to 17 (Table 4, Table E7 [online]). The six additional false-positive results were three non-HCC malignancies (two cHCC-CCAs and one intrahepatic mass-forming cholangiocarcinoma) and three benign lesions (two eosinophilic abscesses and one xanthogranulomatous inflammation). The largest proportion of false-positive results was seen with cHCC-CCAs in both LI-RADS v2017 (eight of 11) and v2018 (10 of 17) (Fig 4). Another notable point was that the false-positive results included benign lesions (one in LI-RADS v2017 and four in LI-RADS v2018) even in patients at high risk for HCCs.

Diagnostic Performance of LR-M in the Diagnosis of Non-HCC Malignancies

LR-M had high specificity (95% [359 of 377]) but lower sensitivity (62% [28 of 45]) in the prediction of non-HCC malignancies (Table E8 [online]) (Fig 5). Furthermore, the sensitivity of LR-M for non-HCC malignancies decreased from 62% (28 of 45) to 38% (three of eight) in 10–19-mm observations, while specificity increased from 95% (359 of 377) to 99% (164 of 165). Among non-HCC malignancies, 27% (four of 15) of cHCC-CCAs, 75% (18 of 24) of intrahepatic mass-forming cholangiocarcinomas, and 100% (six of six) of metastases were accurately categorized as LR-M.

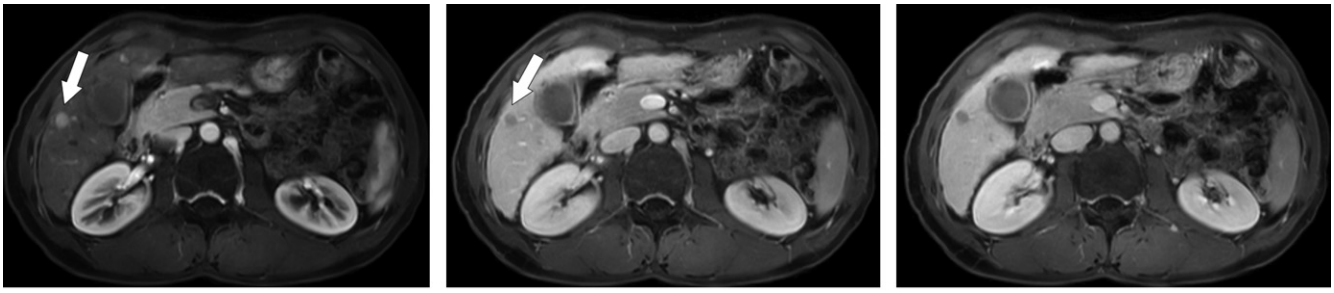

a. b. c.

Figure 3: Axial images at gadoxetate-enhanced MRI in a 55-year-old man with chronic hepatitis B and hepatocelluar carcinoma (HCC). **(a)** Arterial phase, **(b)** portal venous phase, and **(c)** transitional phase T1-weighted three-dimensional gradient-echo images show an 11-mm observation in segment 7 of the liver. The observation shows **(a)** arterial phase hyperenhancement (arrow) and **(b)** washout (arrow) on portal venous phase. Enhancing capsule is not visible on **(b)** portal venous phase and **(c)** transitional phase. This hepatic observation could not be classified as LR-5, but was assigned as LR-4 using Liver Imaging Reporting and Data System (LI-RADS) version 2017. In contrast, this could be categorized as LR-5 using LI-RADS version 2018. It was diagnosed at pathologic examination as HCC.

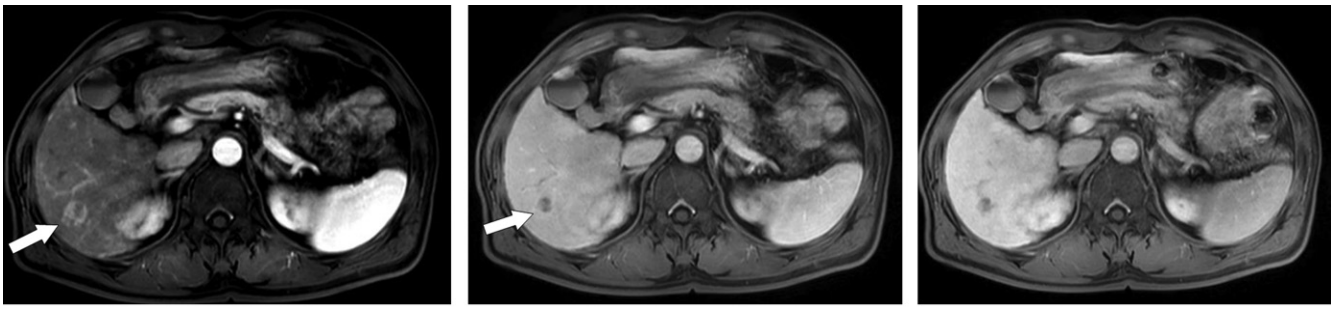

a. b. c.

Figure 4: Axial images at gadoxetate-enhanced MRI in a 59-year-old man with liver cirrhosis and combined hepatocellular carcinoma-cholangiocarcinoma (cHCC-CCA). **(a)** Arterial phase, **(b)** portal venous phase, and **(c)** transitional phase T1-weighted three-dimensional gradient-echo images show a 16-mm observation in segment 6 of the liver. The observation shows **(a)** arterial phase hyperenhancement (arrow) and **(b)** washout (arrow) on the portal venous phase (PVP). An enhancing capsule is not seen on **(b)** PVP and **(c)** the transitional phase. This hepatic observation was additionally categorized as LR-5 by using updated LR-5 criteria of Liver Imaging Reporting and Data Systems version 2018. However, it turned out to be cHCC-CCA after percutaneous biopsy.

Discussion

Liver Imaging Reporting and Data System (LI-RADS) v2018 made several major changes to its algorithm, including updated LR-5 criteria, motivated largely by the goal of aligning the differing diagnostic systems for hepatocellular carcinoma (HCC) and facilitating its integration into the American Association for the Study of Liver Diseases (AASLD) 2018 HCC clinical practice guidelines (7,31). Although previous studies (Table E9 [online]) (8,9,16) had reported that the prior version of LI-RADS was not any better than AASLD in diagnosing small HCCs, we believed LI-RADS v2018 might provide better diagnostic performance than LI-RADS v2017. Indeed, according to our results, the updated LR-5 criteria of LI-RADS v2018 on gadoxetate disodium–enhanced MRI yielded significantly better sensitivity (81%) than LI-RADS v2017 (68%) for the noninvasive diagnosis of HCC. Particularly, in small observations (10–19 mm), sensitivity was much higher with LI-RADS v2018 (76%) compared with LI-RADS v2017 (11%); thirty-one (69%) of 45 small HCCs (10–19 mm) were classified as LR-4, all of which were observations showing arterial phase hyperenhancement (APHE) with only one additional major feature, while 29 small HCCs (10–19 mm) showing APHE and washout were upgraded to LR-5. It should also be noted, however, that specificity was demonstrated to be lower than that of LI-RADS v2017 in all observations (91% vs 94%) and small observations (94% vs 99%).The most common cause of false-positive results was combined HCC-cholangiocarcinoma (cHCC-CCA) in both LI-RADS v2017 (eight of 11) and v2018 (10 of 17).

The better sensitivity of LR-5 criteria of LI-RADS v2018 compared with LI-RADS v2017 in our study was consistent with that of the previous study (19). This better sensitivity of LI-RADS v2018 can be largely attributed to its improved sensitivity for the diagnosis of small HCCs (10–19 mm). The diagnostic performance of LI-RADS v2017 in our study was in agreement with the previous study using LI-RADS v2014 (10). However, in small observations (10–19 mm), LI-RADS v2017 showed poor sensitivity, which was then markedly improved after applying LI-RADS v2018. This was due to changes in LR-5 criteria for the diagnosis of small HCCs (10–19 mm), which require APHE with one additional major feature, including washout or "threshold growth," while excluding the presence of an enhancing capsule, whereas LI-RADS v2017 requires APHE with two additional major features.

The sensitivity (11%) of LR-5 of LI-RADS v2017 using MRI with gadoxetate disodium for the diagnosis of small HCCs

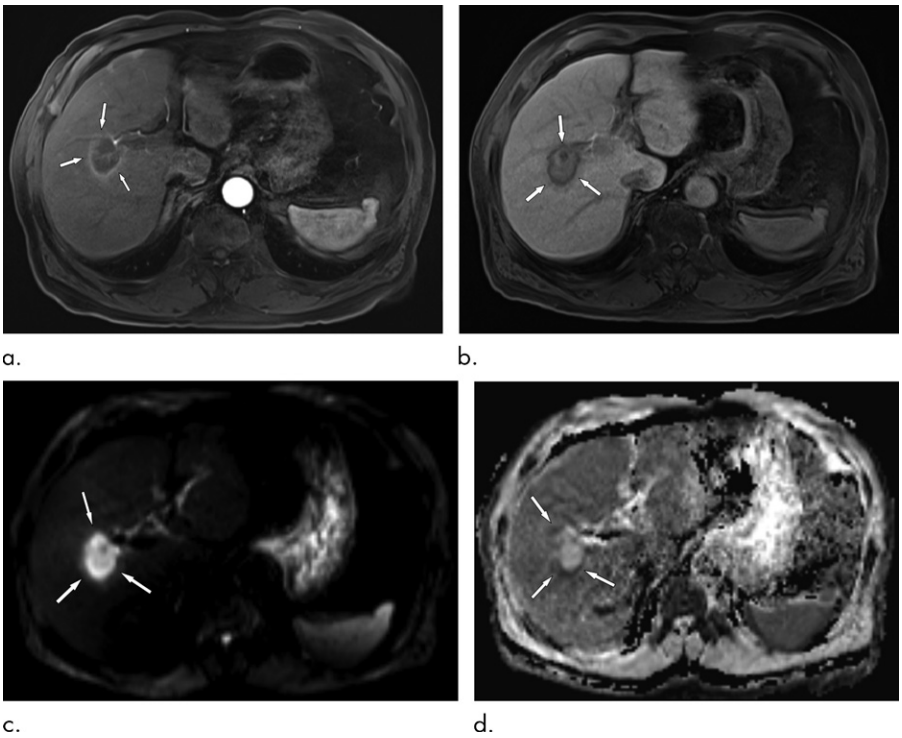

Figure 5: Axial images at gadoxetate-enhanced MRI in an 81-year-old man with liver cirrhosis and intrahepatic mass-forming cholangiocarcinoma (IMCC). **(a)** Arterial phase and **(b)** hepatobiliary phase T1-weighted three-dimensional gradient-echo images show a 36-mm observation in segment 5/8 of the liver. The observation shows **(a)** rim arterial phase hyperenhancement (arrows) and **(b)** targetoid appearance (arrows) on hepatobiliary phase. **(c)** High-*b*-value (*b* = 800 sec/mm^2) diffusion-weighted image and **(d)** apparent diffusion coefficient map show targetoid restriction (arrows). This hepatic observation was categorized as LR-M. It was confirmed as IMCC at percutaneous biopsy.

(10–19 mm) in our study was much lower than that (42%) obtained in the study using MRI with ECA (9). This lower sensitivity of MRI with gadoxetate disodium for small HCCs could be attributed to the unavailability of "visibility at screening ultrasound" or "threshold growth," the use of only portal venous phase for determining the washout appearance, and lower depiction of the capsule appearance on portal or 3-minute–delayed scans compared with MRI with ECA (14,32). The studies comparing MRI with ECA versus MRI with gadoxetate disodium by using LI-RADS v2014 or v2017 demonstrated that the sensitivity for LR-5 using MRI with gadoxetate disodium was lower than that using MRI with ECA (13,14). According to the study by Song et al (14), it was associated with the lower depiction of washout (61% vs 77%) and the capsule appearance (51% vs 75%). To the contrary, the diagnostic performance of LR-5 of LI-RADS v2018 using liver MRI with gadoxetate disodium in our study was at least comparable to that in previous studies using liver MRI with ECA. Therefore, further comparison studies between ECA and gadoxetate disodium would be warranted as the changes in the LR-5 criteria of LI-RADS v2018 may have affected the diagnostic performance of liver MRI with ECA or gadoxetate disodium.

It should also be noted in our study, however, that LI-RADS v2018 showed decreased specificity in the diagnosis of HCCs compared with LI-RADS v2017 although it did maintain a specificity over 90% according to the consensus data (82%–94% from per-reader data). The ideal specificity would depend on the selected strategy for treatment of patients with HCCs. Nevertheless, a decrease in specificity means an increase in false-positive results. In other words, more benign lesions and non-HCC malignancies could be diagnosed as HCCs even in patients at high risk for HCC and these patients may receive treatments such as liver transplantations, resections, or local-regional therapy without biopsy because imaging-based diagnosis of HCC can be allowed in high-risk patients. Therefore, the lower specificity of LI-RADS v2018 may lead to overtreatment of HCCs, and organ allocation for liver transplantation may also be a big concern. Fortunately, organizations such as the Organ Procurement and Transplantation Network would not give priority for single HCCs smaller than 2 cm for patients on the waiting list for liver transplantations.

Our results demonstrated that the most common cause of false-positive results with LR-5 was cHCC-CCA; this was consistent with results of previous studies (10,23). Several studies also demonstrated that some cHCC-CCAs could not be differentiated from HCCs based on imaging features (10,33). Although there have been controversies regarding the prognosis of patients with cHCC-CCAs after surgical resection or liver transplantation, compared with the prognosis of patients with HCCs, recent studies demonstrated that most patients with small or early stage cHCC-CCAs might have similar survival after surgical treatment (34,35).

Our study has several limitations. First, we conducted our study retrospectively at a single center, and more than half of the eligible patients were excluded due to lack of a reference standard for their diagnosis. Second, only 18 of 143 benign lesions were confirmed with pathologic examination, although in the actual clinical setting the pathologic diagnosis of a benign lesion would be required when the imaging features are atypical. This may have caused selection bias. Third, we did not consider ancillary features in LR-5, LR-TIV, or LR-M categorization. However, ancillary features cannot be used to upgrade to LR-5 and did not affect the diagnostic performance of LR-5 for the noninvasive diagnosis of HCC. Fourth, there were only 45 small HCCs (10–19 mm), as

many small HCCs were treated through local-regional treatment after having noninvasive diagnosis based on imaging features at our center. Finally, we did not evaluate visibility at screening US and threshold growth, which might have caused alteration of the sensitivity of LR-5 in the diagnosis of HCC.

In conclusion, the updated LR-5 criteria of Liver Imaging Reporting and Data System (LI-RADS) version 2018 on gadoxetate disodium–enhanced MRI can improve sensitivity for the diagnosis of small hepatocelluar carcinomas (10–19 mm) compared with LI-RADS version 2017, albeit with slight impairment in specificity.

Acknowledgments: The authors would like to thank Professor Junhee Han, Department of Statistics and Institute of Statistics, Hallym University, for his statistical assistance. The statistical analysis of this study was also supported by the Division of Biostatistics, Hallym Institute for Clinical Medicine, Hallym University Medical Center.

Author contributions: Guarantors of integrity of entire study, J.M.L., H.J.K.; study concepts/study design or data acquisition or data analysis/interpretation, all authors; manuscript drafting or manuscript revision for important intellectual content, all authors; approval of final version of submitted manuscript, all authors; agree to ensure any questions related to the work are appropriately resolved, all authors; literature research, S.M.L., J.M.L., J.H.Y.; clinical studies, S.M.L., J.M.L., S.J.A., H.J.K., H.K.Y.; statistical analysis, S.M.L., H.J.K.; and manuscript editing, S.M.L., J.M.L., J.H.Y.

Disclosures of Conflicts of Interest: **S.M.L.** disclosed no relevant relationships. **J.M.L.** Activities related to the present article: disclosed no relevant relationships. Activities not related to the present article: disclosed institutional grants from RF Medical, Bayer Healthcare, Guerbet, Samsung Medison, Philips Healthcare, GE Healthcare, CMS, and Canon Healthcare; and receipt of payment from Siemens Healthcare, Guerbet, and Bayer Healthcare for lectures, including service on speakers' bureaus. Other relationships: disclosed no relevant relationships. **S.J.A.** disclosed no relevant relationships. **H.J.K.** disclosed no relevant relationships. **H.K.Y.** disclosed no relevant relationships. **J.H.Y.** Activities related to the present article: disclosed no relevant relationships. Activities not related to the present article: disclosed receipt of payment from Samsung Electronics for consultancy, institutional grant from Bayer, and receipt of payment from Philips Healthcare and Bayer for lectures, including service on speakers' bureaus. Other relationships: disclosed no relevant relationships.

References

1. Heimbach JK, Kulik LM, Finn RS, et al. AASLD guidelines for the treatment of hepatocellular carcinoma. Hepatology 2018;67(1):358–380.
2. Kim TH, Kim SY, Tang A, Lee JM. Comparison of international guidelines for noninvasive diagnosis of hepatocellular carcinoma: 2018 update. Clin Mol Hepatol 2019 Feb 14 [Epub ahead of print] https://doi.org/10.3350/cmh.2018.0090.
3. Tang A, Cruite I, Sirlin CB. Toward a standardized system for hepatocellular carcinoma diagnosis using computed tomography and MRI. Expert Rev Gastroenterol Hepatol 2013;7(3):269–279.
4. Santillan C, Chernyak V, Sirlin C. LI-RADS categories: concepts, definitions, and criteria. Abdom Radiol (NY) 2018;43(1):101–110.
5. Shah A, Tang A, Santillan C, Sirlin C. Cirrhotic liver: What's that nodule? The LI-RADS approach. J Magn Reson Imaging 2016;43(2):281–294.
6. Kim BR, Lee JM, Lee DH, et al. Diagnostic performance of gadoxetic acid-enhanced liver MR imaging versus multidetector CT in the detection of dysplastic nodules and early hepatocellular carcinoma. Radiology 2017;285(1):134–146.
7. Chernyak V, Fowler KJ, Kamaya A, et al. Liver Imaging Reporting and Data System (LI-RADS) Version 2018: imaging of hepatocellular carcinoma in at-risk patients. Radiology 2018;289(3):816–830.
8. Ronot M, Fouque O, Esvan M, Lebigot J, Aubé C, Vilgrain V. Comparison of the accuracy of AASLD and LI-RADS criteria for the non-invasive diagnosis of HCC smaller than 3 cm. J Hepatol 2018;68(4):715–723.
9. Darnell A, Forner A, Rimola J, et al. Liver Imaging Reporting and Data System with MR Imaging: evaluation in nodules 20 mm or smaller detected in cirrhosis at screening US. Radiology 2015;275(3):698–707.
10. Fraum TJ, Tsai R, Rohe E, et al. Differentiation of hepatocellular carcinoma from other hepatic malignancies in patients at risk: diagnostic performance of the Liver Imaging Reporting and Data System Version 2014. Radiology 2018;286(1):158–172.
11. Cerny M, Bergeron C, Billiard JS, et al. LI-RADS for MR imaging diagnosis of hepatocellular carcinoma: performance of major and ancillary features. Radiology 2018;288(1):118–128.
12. Kierans AS, Makkar J, Guniganti P, et al. Validation of Liver Imaging Reporting and Data System 2017 (LI-RADS) criteria for imaging diagnosis of hepatocellular carcinoma. J Magn Reson Imaging 2018 Sep 26 [Epub ahead of print] https://doi.org/10.1002/jmri.26329.
13. Min JH, Kim JM, Kim YK, et al. Prospective intraindividual comparison of magnetic resonance imaging with gadoxetic acid and extracellular contrast for diagnosis of hepatocellular carcinomas using the Liver Imaging Reporting and Data System. Hepatology 2018;68(6):2254–2266.
14. Song JS, Choi EJ, Hwang SB, Hwang HP, Choi H. LI-RADS v2014 categorization of hepatocellular carcinoma: intraindividual comparison between gadopentetate dimeglumine-enhanced MRI and gadoxetic acid-enhanced MRI. Eur Radiol 2019;29(1):401–410.
15. Choi SH, Byun JH, Kim SY, et al. Liver Imaging Reporting and Data System v2014 with gadoxetate disodium-enhanced magnetic resonance imaging: validation of LI-RADS category 4 and 5 criteria. Invest Radiol 2016;51(8):483–490.
16. Yoon JH, Lee JM, Lee YJ, Lee KB, Han JK. Added value of sequentially performed gadoxetic acid-enhanced liver MRI for the diagnosis of small (10-19 mm) or atypical hepatic observations at contrast-enhanced CT: a prospective comparison. J Magn Reson Imaging 2019;49(2):574–587.
17. Stigliano R, Burroughs AK. Should we biopsy each liver mass suspicious for HCC before liver transplantation?--no, please don't. J Hepatol 2005;43(4):563–568.
18. Stigliano R, Marelli L, Yu D, Davies N, Patch D, Burroughs AK. Seeding following percutaneous diagnostic and therapeutic approaches for hepatocellular carcinoma. What is the risk and the outcome? Seeding risk for percutaneous approach of HCC. Cancer Treat Rev 2007;33(5):437–447.
19. Ren AH, Zhao PF, Yang DW, Du JB, Wang ZC, Yang ZH. Diagnostic performance of MR for hepatocellular carcinoma based on LI-RADS v2018, compared with v2017. J Magn Reson Imaging 2019 Jan 15 [Epub ahead of print] https://doi.org/10.1002/jmri.26640.
20. Kim YY, Kim MJ, Kim EH, Roh YH, An C. Hepatocellular carcinoma versus other hepatic malignancy in cirrhosis: performance of LI-RADS version 2018. Radiology 2019;291(1):72–80.
21. Ludwig DR, Fraum TJ, Cannella R, et al. Hepatocellular carcinoma (HCC) versus non-HCC: accuracy and reliability of Liver Imaging Reporting and Data System v2018. Abdom Radiol (NY) 2019;44(6):2116–2132.
22. American College of Radiology. Liver Reporting and Data System version 2017. https://www.acr.org/Clinical-Resources/Reporting-and-Data-Systems/LI-RADS/CT-MRI-LI-RADS-v2017. Accessed June 27, 2017.
23. Joo I, Lee JM, Lee DH, Jeon JH, Han JK, Choi BI. Noninvasive diagnosis of hepatocellular carcinoma on gadoxetic acid-enhanced MRI: can hypointensity on the hepatobiliary phase be used as an alternative to washout? Eur Radiol 2015;25(10):2859–2868.
24. Tang A, Bashir MR, Corwin MT, et al. Evidence supporting LI-RADS major features for CT- and MR imaging-based diagnosis of hepatocellular carcinoma: a systematic review. Radiology 2018;286(1):29–48.
25. Oto A, Kulkarni K, Nishikawa R, Baron RL. Contrast enhancement of hepatic hemangiomas on multiphase MDCT: can we diagnose hepatic hemangiomas by comparing enhancement with blood pool? AJR Am J Roentgenol 2010;195(2):381–386.
26. Ahn JH, Yu JS, Hwang SH, Chung JJ, Kim JH, Kim KW. Nontumorous arterioportal shunts in the liver: CT and MRI findings considering mechanisms and fate. Eur Radiol 2010;20(2):385–394.
27. Hussain SM, Reinhold C, Mitchell DG. Cirrhosis and lesion characterization at MR imaging. RadioGraphics 2009;29(6):1637–1652.
28. Grieser C, Steffen IG, Seehofer D, et al. Histopathologically confirmed focal nodular hyperplasia of the liver: gadoxetic acid-enhanced MRI characteristics. Magn Reson Imaging 2013;31(5):755–760.
29. Byun JH, Yang DH, Yoon SE, et al. Contrast-enhancing hepatic eosinophilic abscess during the hepatic arterial phase: a mimic of hepatocellular carcinoma. AJR Am J Roentgenol 2006;186(1):168–173.
30. Landis JR, Koch GG. The measurement of observer agreement for categorical data. Biometrics 1977;33(1):159–174.
31. Marrero JA, Kulik LM, Sirlin CB, et al. Diagnosis, Staging, and Management of Hepatocellular Carcinoma: 2018 Practice Guidance by the American Association for the Study of Liver Diseases. Hepatology 2018;68(2):723–750.
32. Dioguardi Burgio M, Picone D, Cabibbo G, Midiri M, Lagalla R, Brancatelli G. MR-imaging features of hepatocellular carcinoma capsule appearance in cirrhotic liver: comparison of gadoxetic acid and gadobenate dimeglumine. Abdom Radiol (NY) 2016;41(8):1546–1554.
33. Jeon SK, Joo I, Lee DH, et al. Combined hepatocellular cholangiocarcinoma: LI-RADS v2017 categorisation for differential diagnosis and prognostication on gadoxetic acid-enhanced MR imaging. Eur Radiol 2019;29(1):373–382.
34. Wu CH, Yong CC, Liew EH, et al. Combined hepatocellular carcinoma and cholangiocarcinoma: diagnosis and prognosis after resection or transplantation. Transplant Proc 2016;48(4):1100–1104.
35. Jung DH, Hwang S, Song GW, et al. Longterm prognosis of combined hepatocellular carcinoma-cholangiocarcinoma following liver transplantation and resection. Liver Transpl 2017;23(3):330–341.